Journal of Structural Geology, Vol. 8, No. 6, pp. 669 to 681, 1986
Printed in Great Britain

0191-8141/86 $03.00 + 0.00
Pergamon Journals Ltd.

Cataclastic deformation of quartzite in the Moine thrust zone

T. G. BLENKINSOP* and E. H. RUTTER

Department of Geology, Royal School of Mines, Imperial College of Science and Technology, London, SW7 2BP, England

(*Received* 25 *February* 1985; *accepted in revised form* 11 *November* 1985)

Abstract—Deformed Cambrian quartzites from the Moine thrust zone on Skye have been examined under cathodoluminescence in the Scanning Electron Microscope (SEM). A sequence of progressive deformation from intact quartzite through protobreccia to breccia and ultrabreccia can be established for samples from a large fold with a wavelength of 2 km, and a comparable cataclasite sequence exists for samples approaching the Ord thrust plane. The microstructural evolution involves the development of extension microcracks by impingement at grain contacts, followed by the formation of small shear faults by linking of the extension microcracks. Further strain is localized on large breccia zones; the proportion of fine-grained matrix increases and fluid flow is concentrated into the dilatant zones, depositing cement and iron oxides. The dominant deformation mechanism for both folding and faulting in this part of the Moine thrust zone is cataclasis. Extension microcracks and shear faults have close analogues in experimental deformation, but the formation of the protobreccia in the hinge of the fold is an example of cataclastic flow on a much larger scale than a laboratory specimen. The conditions for the initiation of the shear faults and breccia zones are suggested by the Rudnicki and Rice model of a dilatant material. Work-hardening must occur in both cases; possible mechanisms include changes in the dilatancy factor and bulk modulus, and syntectonic cementation.

INTRODUCTION

A WEALTH of experimental data and observation exists on specimens deformed by cataclasis in the laboratory, including the results of triaxial testing to brittle failure, creep tests, determinations of frictional sliding and fault gouge rheology, studies of 'semibrittle' behaviour, and more recently, investigations to determine fracture toughness and sub-critical crack growth parameters using the methods of fracture mechanics (e.g. Paterson 1978 for a review of many of these aspects). This is complemented by a growing volume of literature on field and microstructural observations of natural cataclasites, including the work of Stearns (1968), Engelder (1974), Brock & Engelder (1977), House & Gray (1982), Hadizadeh & Rutter (1982), Robertson (1982, 1983), Jamison & Stearns (1982) and Aydin & Johnson (1983). Several attempts have also been made to derive theoretical models of cataclasis, such as those of Peng & Johnson (1972), Cruden (1974), Brady (1974), Rudnicki & Rice (1975), Wilkins (1980), Aydin & Johnson (1983) and Costin (1983). However, compared to deformation by intracrystalline plasticity, with certain exceptions (e.g. Engelder 1974) little has been done to address the important question of the extent to which cataclasites in nature behave similarly to the laboratory experiments or theoretical models. Hadizadeh & Rutter (1982) have indicated that there may be serious problems of scale in extrapolating from the results of a conventional triaxial test to crustal deformation.

The aims of this study are to describe natural examples of cataclasis from both a fault and a fold, to elucidate its microstructural evolution in detail, and to make some comparisons with experimental and theoretical results.

METHODS OF STUDY

The southwestern part of the Moine thrust zone on Skye was mapped at a scale of 1:10,000 around the Ord thrust, Sgiath Bheinn Tokavaig antiform, Tarskavaig thrust and Tarskavaig synform (Fig. 1). The samples for this study were collected from around the hinge and limb of the Sgiath Bheinn Tokavaig antiform and along the Ord thrust plane (Fig. 2), and examined in conventional optical microscopy and by cathodoluminescence in the Scanning Electron Microscope (SEM). Grain size and microcrack lengths from the sections were measured by linear intercepts from traces on thin sections, and microcrack orientations determined from two mutually perpendicular thin sections. Microcrack densities, also determined from two perpendicular thin sections, were measured by linear intercepts along a line perpendicular to the preferred orientation of crack traces. A correction was then applied to this figure to allow for the obliquity of the crack planes relative to the plane of sections. The figures reported therefore approximate to the reciprocal of the crack spacing. X-ray diffraction on the clay fraction of samples from the Fucoid Beds and the Torridonian sediments (Fig. 1) was used to determine the mineralogy, and an estimate of temperature was made from illite crystallinity. The relative importance of intracrystalline plasticity was evaluated from a quantitative study of undulatory extinction.

* Present address: Department of Geology, University of Keele, Keele, Staffs, ST5 5BG, England.

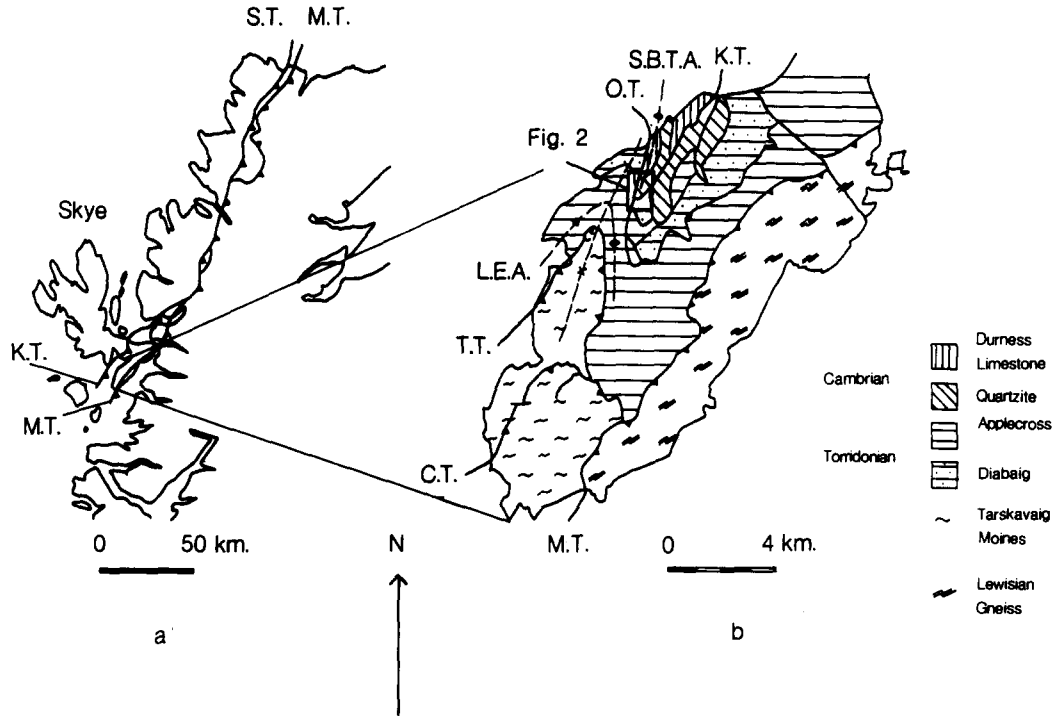

Fig. 1. (a) The Moine thrust zone in Scotland. M.T., Moine thrust; K.T., Kishorn thrust; S.T., Sole thrust. (b) Geology of the Sleat peninsula, Skye. M.T., Moine thrust; C.T., Caradal thrust; K.T., Kishorn thrust; T.T., Tarskavaig thrust; O.T., Ord thrust; T.S., Tarskavaig synform; L.E.A., Loch Eishort antiform; S.B.T.A., Sgiath Bheinn Tokavaig antiform.

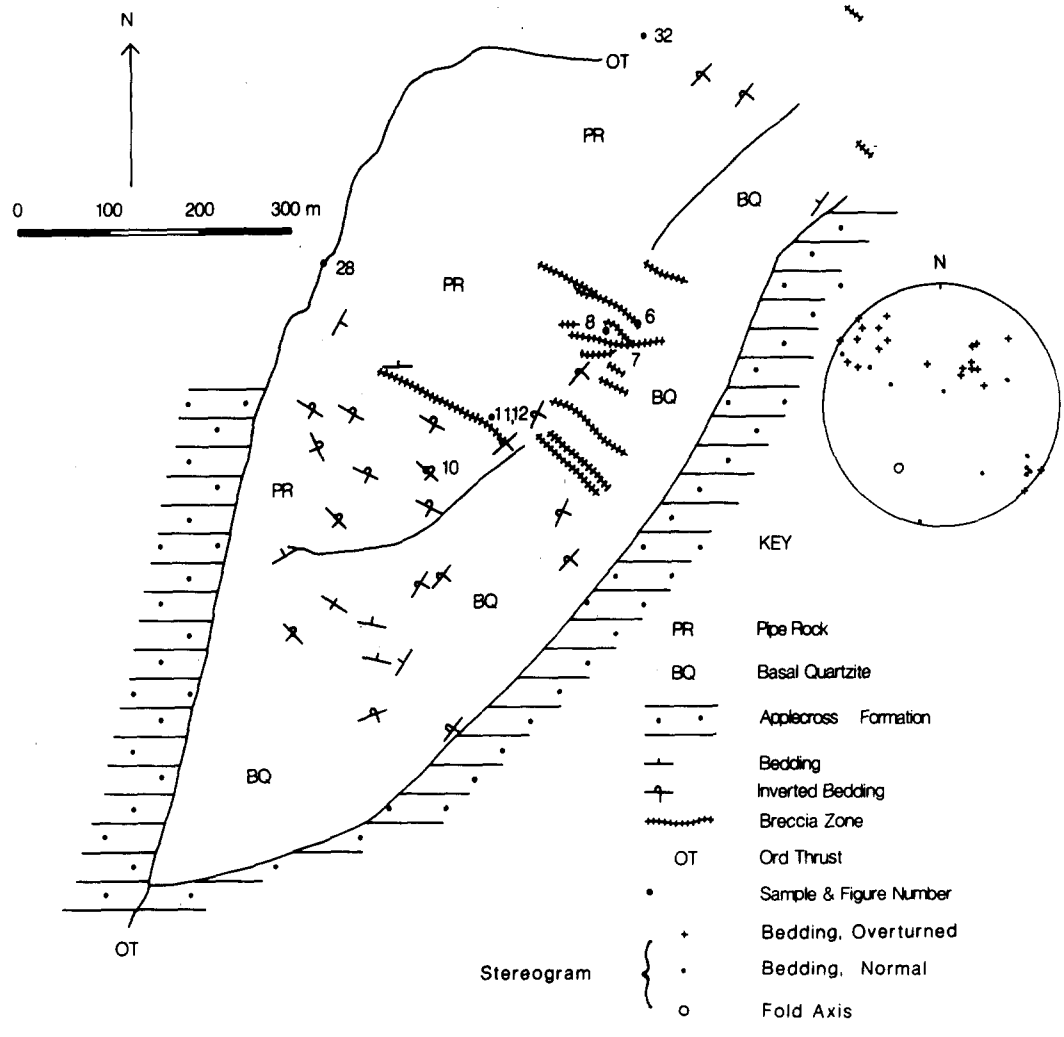

Fig. 2. Detailed map of sample area, showing sample locations. Stereogram (equal area, lower hemisphere projection) shows poles to bedding. Bed dips are generally steep. The fold axis plunges at 36° to 217.

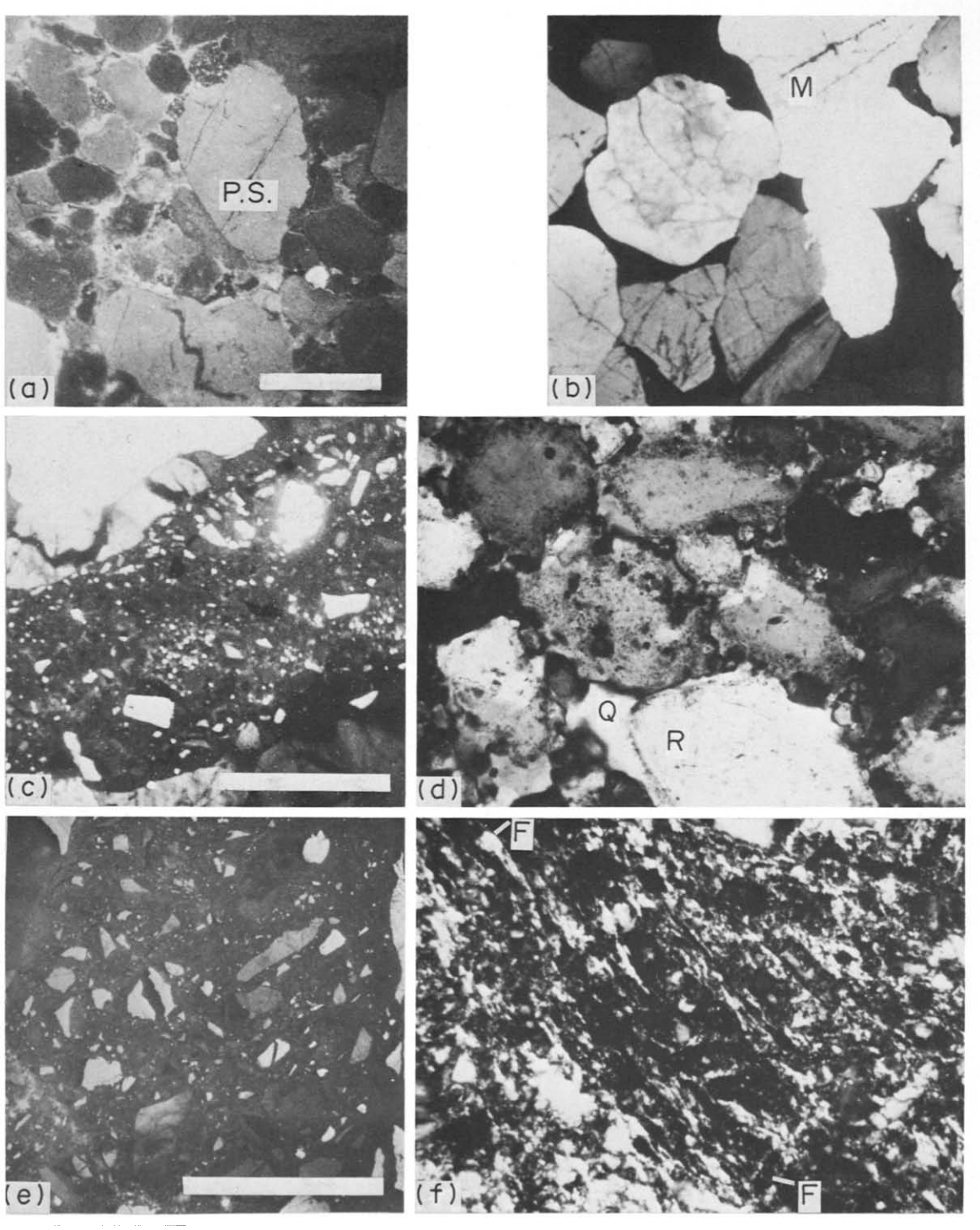

Fig. 3. (a) Intact quartzite (sample 32). Variable luminescence and inherited structures of grains can be seen under CL. A typical pressure solution grain boundary (P.S.) can be seen at the centre of the figure. (b) Protobreccia (sample 12). Intragranular extension microcracks (M) show up clearly in CL as lines of non-luminescing quartz. (c) Protobreccia (sample 12). A small shear fault crosses the figure, filled with fine-grained, non-luminescing matrix and crushed fragments of grains; under CL. (d) Breccia (sample 6). Iron oxide rims (R) and optically continuous quartz overgrowths (Q) surround most grains. Optical thin section, crossed polars. (e) Ultrabreccia (sample 7). Typical texture of complete reduction of grains to small round fragments, surrounded by fine grained matrix; under CL. (f) Ultracataclasite (sample 28) from the Ord thrust plane. A foliation (F) is defined by micas in a matrix of completely reduced fragments and cement. Optical thin section, crossed polars. Scale bar in all photomicrographs is 200 μm. See Fig. 2 for sample locations.

THE APPLICATION OF CATHODOLUMINESCENCE TO THE STUDY OF ROCKS DEFORMED NATURALLY BY CATACLASIS

The first modern petrological studies using Cathodoluminescence (CL) were made by Sipple (1968), Smith & Stenstrom (1965) and Long & Agrell (1965). These workers all used a CL device similar to that of Sipple (1968), in which the luminescence of minerals under a broad electron beam from a cold cathode source was observed directly in a petrological microscope. The development of the Scanning Electron Microscope (SEM), involving the generation of a narrow, dense electron beam, suggested a ready conversion to the CL mode: such a device was made in the early 1970s by, for example, Muir & Holt (1974).

The quartz grains of the sample are excited by the electron beam of the SEM which detects the luminescence of each point under the beam with a photomultiplier. Photographs of the luminescence can be taken as the beam scans across the whole field, or spectral analysis may be made by placing a grating monochromator in front of the photomultiplier (Zinkernagel 1978).

The variation in luminescence amplitude and wavelength has been attributed to a number of different causes for different minerals. The theory of activator luminescence was strongly supported by the work of Sommers (1972), which showed that luminescence in a variety of carbonates correlated precisely with the Mn:Fe ratio. The luminescence can be explained by quantum jumps in the f- and d-orbitals of Mn, which is referred to as an activator. However, it has proved impossible to identify activator elements in quartz, for which an alternative theory of lattice luminescence was proposed by Zinkernagel (1978). Lattice defects are a possible source of luminescence, which will thus depend on the silica polymorph and its thermal and mechanical history (e.g. Smith & Stenstrom 1965, Sprunt *et al.* 1978). Healed microcracks in quartz in granitic rocks appear as lines of red luminescing quartz in blue host grains (Sprunt & Nur 1979). The latter authors inferred that the crack fillings were made at a lower temperature than that of the crystallization of the granites.

The technique of CL can reveal important features of cataclastically deformed rocks that are not visible optically. In optical microscopy, trails of bubbles may be seen along microcrack margins like those illustrated by Knipe & White (1979) from shear zones in sandstone. In the present study, however, CL sharply delineated the entire microcrack fill as non-luminescing quartz and led to the identification of the bubble trails as cracks. Cement in the fine grained matrix of shear faults is also shown as non-luminescing quartz. The different origins and thermo-mechanical histories of quartz which appears optically continuous can be distinguished by the CL technique as shown in the luminescence images in Figs. 3(a–c & e).

THE MOINE THRUST ZONE ON SKYE

Skye is at the southern end of the Moine thrust zone, the outcrop width of which is here greater than 10 km, and consists of a number of thrusts carrying nappes towards the northwest (McClay & Coward 1982 and Fig. 1). A schematic cross-section of the five thrusts and nappes exposed at the south end of Skye is shown in Fig. 4. With the exception of late movements on the Moine thrust, this succession can also be regarded as the order of thrust emplacement, giving a conventional foreland propagating sequence (Potts 1982, Butler 1982). However, the interrelationships of the thrusts and folds are not obvious and have been interpreted in several different ways (Cheeney & Matthews 1965, Potts 1982).

Deformation by both folding and thrusting at the southern end of the outcrop of the Moine thrust zone, for example on Skye, is dominated by cataclastic processes. By contrast, at the northern end of the outcrop (north coast of Scotland), plastic deformation is dominant, though localized zones of cataclasis are developed during the evolution of the displacements in the thrust zone. This broad spatial transition in deformation mechanism may reflect a greater degree of uplift at the northern end of the zone.

The low grade metamorphic conditions on Sleat (see Fig. 1a for location) are particularly difficult to describe

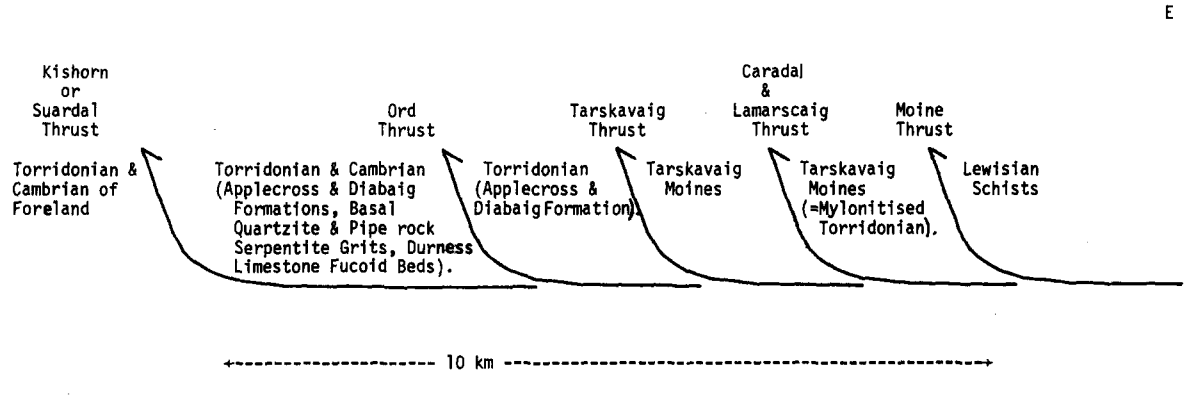

Fig. 4. Schematic section of the thrusts and nappe rocks of the Moine thrust zone on the Sleat peninsula, Skye.

accurately. At no place in the south of the peninsula has cleavage developed in any rock type, and quartz grains in the folded rocks show no signs of crystal plasticity. Temperatures may therefore have reached no more than 200°C (White 1976). The X-ray diffraction analysis of the associated Fucoid Beds showed a mineral assemblage of illite, chlorite, kaolinite and traces of vermiculite–mixed layer chlorite. The illite crystallinity gave a metamorphic grade on the diagenetic–anchizone (Kisch 1983) boundary, confirming the inferred upper temperature limit. For an average continental geotherm, this constrains the maximum depth to be about 7 km. The stratigraphic thickness above the base of the Cambrian quartzites within the Kishorn nappe (Figs. 1 and 4) is 900 m.

FIELD AND MICROSCOPE OBSERVATIONS OF THE QUARTZITE

Quartzites on the hinge and limb of the Sgiath Bheinn Tokavaig antiform (Figs. 1 and 2) have been classified into four types from both field and microscopic observations: (a) *intact quartzite*; (b) *protobreccia*; (c) *breccia*; (d) *ultrabreccia*. These terms are introduced to clarify the distinction between the *description* of various textural types and the *process* by which they were formed (cataclasis). The suffix 'breccia' emphasizes the significant point that the macroscopically *pervasive* strains within the Sgiath Bheinn Tokavaig antiform are accommodated by a brittle process in contrast to the often very *localized* strains accommodated by cataclasites along major fault planes. This nomenclature has some features in common with the "suggestions for terminology" for fault related rocks made by Wise *et al.* (1984), but it deliberately avoids making possibly difficult inferences about strain and recovery rates. It serves merely to facilitate the description of the rocks and is not intended as a comprehensive classification of fault rocks.

(a) Intact quartzite

The relatively undeformed quartzite contains angular to sub-rounded detrital grains with an average diameter of 0.2 mm which interlock on curved or irregular grain boundaries due to a limited amount of tectonic pressure solution. CL reveals that the grains have a wide variety of provenances and show inherited substructures such as patchy luminescence intensity which is indicative of their lithic character (Fig. 3a).

(b) Protobreccia

A protobreccia is defined as containing more than 75% of intact quartzite fragments in a fine grained matrix. In the field one sees lozenge shaped tablets of intact rock bounded by sub-parallel fractures about 5 cm long with a spacing of 1–2 cm. The whole rock is commonly stained red or yellow. Microscopically, two types of failure can be distinguished in these rocks on the basis of size and mode of occurrence.

(i) Extension microcracks. These are generally a few μm wide and have purely extensional displacements, occurring mostly as intragranular cracks (Fig. 3b). They are invariably filled with quartz in optical continuity with the host fragments. Histograms of microcrack lengths (Fig. 5) show that the mean length is always less than the grain diameter. Those that traverse the greater part of a grain diameter have a good preferred orientation (Fig. 6) whereas cracking is more intense at impingement points between grains, from which smaller cracks radiate. This type of damage is not evident in the field because the crack fill is structurally contiguous with the

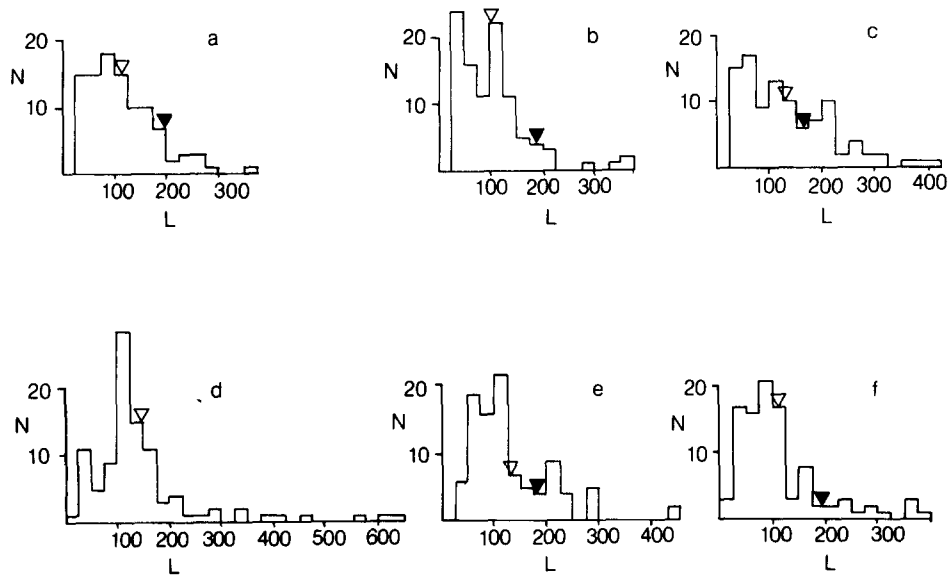

Fig. 5. Histograms of extension microcrack length L (μm). N, number of microcracks; open triangle, mean microcrack length, $\bar{L}$, for each sample; closed triangle, mean linear intercept, D, of grain size for each sample. 100 measurements for each sample; $\bar{L}$ is approximately constant and always less than D. (a) Intact quartzite (sample 32); (b) protobreccia (sample 11); (c) protobreccia (sample 10); (d) protobreccia (sample 8), (e) breccia (sample 6) and (f) ultrabreccia (sample 7). See Fig. 2 for sample locations.

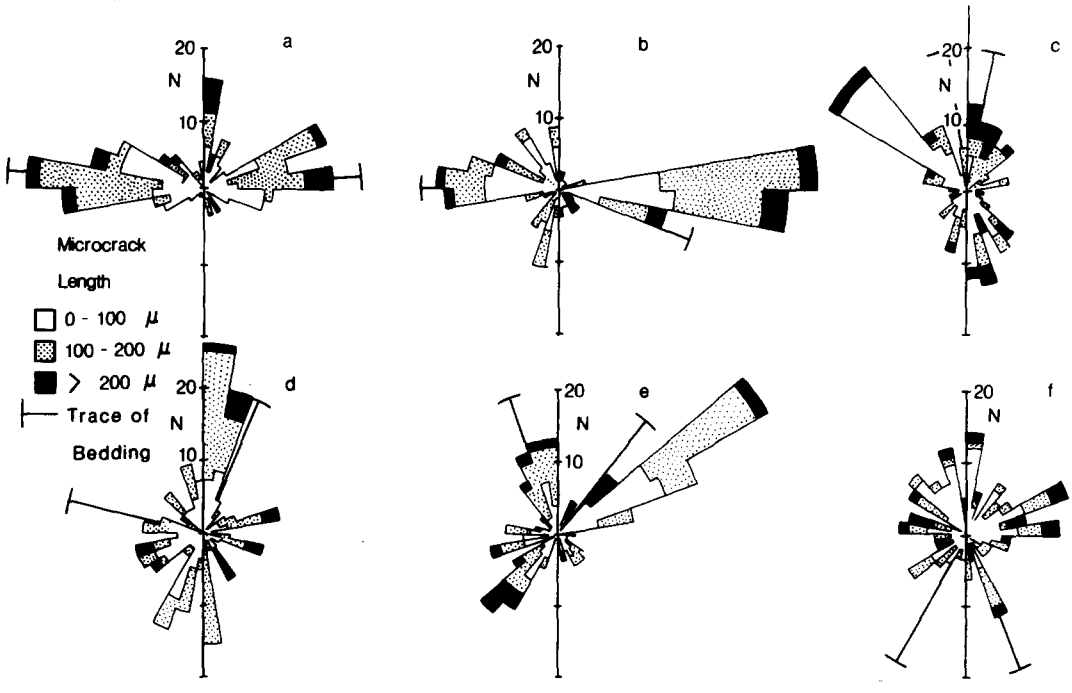

Fig. 6. Rose diagrams of extension microcrack orientations and lengths in the plane of section. Each half of the rose diagram shows measurements from one of a pair of perpendicular thin sections, and shows the trace of bedding in the section. The two sections join along the vertical diameter of the figure. The poles to mean extension microcrack orientations can be deduced from this figure and the known orientations of the sections, and are shown in Fig. 7. 100 measurements for each section. All the samples show a good preferred orientation with the exception of the ultrabreccia. (a) Intact quartzite (sample 32); (b) protobreccia (sample 11); (c) protobreccia (sample 10); (d) protobreccia (sample 8); (e) breccia (sample 6) and (f) ultrabreccia (sample 7). See Fig. 2 for sample locations.

host grain. Between the shear faults (below) the rock appears intact. The intergranular cement is often uncracked, and, like the intragranular crack fill, is non-luminescent. Thus these earlier stages of deformation were probably accomplished when the rock was less cemented than it appears now.

(ii) Shear faults. These are from 1 to 4 mm wide and are filled with a fine-grained matrix consisting of fragmented grains, iron oxides, and non-luminescing cement (Fig. 3c). They are generally a few centimetres long with displacements of several millimetres, and can be identified as the same faults that isolate the lozenge-shaped tablets of intact rock which can be perceived in the field. Their edges are usually straight, and they too have a good preferred orientation. The mean orientations of extension microcracks compared to shear faults and breccia zones (below) is shown in Fig. 7 together with the fold axis orientation. The microcracks, shear faults and breccia zones show a tendency to lie at a high angle to the fold axis, but there is no indication that these features have been rotated about the fold axis. Their development is probably broadly coeval with folding. The microcrack arrays tend to intersect associated shear faults and breccia zones at large angles however, often approaching 90°, even in parts of the protobreccia remote from any rotation occurring on the shear faults.

The texture of the protobreccias thus consists of a network of sub-parallel shear faults separating fragments of 'intact' quartzite which are damaged by intragranular extension microcracks.

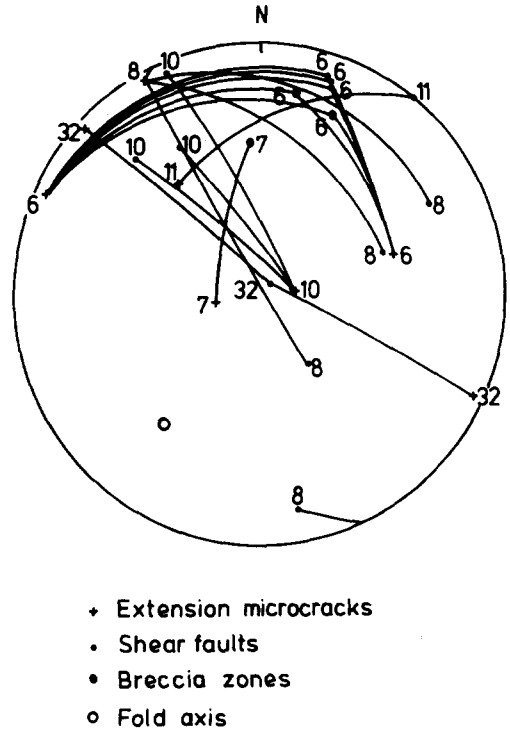

Fig. 7. Poles to extension microcracks (measured from data of Fig. 6), shear faults and breccia zones on the hinge and limb of the Sgiath Bheinn Tokavaig antiform. The poles to the microcracks have been joined to the poles of shear faults or breccia zones in the same sample along great circles. Large angles are subtended between the microcracks and shear faults or breccia zones, and both tend to make a large angle with the fold axis, but the faults are not systematically rotated around the fold axis. See Fig. 2 for sample locations. Lower hemisphere, equal-area projection.

(c) Breccia

A further degree of damage is perceived in the breccias, in which the proportion of lithic fragments is reduced to between 25 and 75% (by definition) with a concomitant increase in the proportion of matrix. The high concentration of iron oxides in the matrix gives this rock a deep red colour. Breccias outcrop in straight, vertical planar zones 1–200 m long, intersecting the Ord thrust at 80–90° (Fig. 2). They have widths of 2–150 cm, which vary extremely abruptly along their lengths. The size of angular fragments within the breccia reflects to some extent the width of the breccia zone at that point. No estimate of displacement across an individual breccia was possible: bedding becomes obscured in the vicinity of the breccias. The outcrop of the Basal Quartzite–Pipe-Rock boundary shown in Fig. 2 suggests that displacements of the order of metres at most are associated with the breccia zones.

Microscopically, intragranular extension microcracks of the same length and distribution as those in the protobreccia are developed (Fig. 5), although their density has increased (Table 1). An important additional observation is that intact grains have a rim of iron oxide inclusions surrounded by an optically continuous overgrowth in all directions, which is up to 50 μm wide (Fig. 3c). Breccias are distinguished from protobreccias on the basis of both their microstructural character and their field relations. They form in discrete zones which represent heterogeneities at an outcrop scale with a spacing of 1–50 m, and they have greater microcrack densities, and higher proportions of sheared matrix and iron oxides than the protobreccias.

(d) Ultrabreccia

Locally within the breccia zones, the proportion of relatively intact fragments is reduced to less than 25%, thus defining an ultrabreccia. The whole rock is now distinctly matrix supported. These fragments are smaller and more rounded (Fig. 3e). Due to the small proportion of 'intact' fragments, few microcracks are preserved in the ultrabreccias. Those present have the same mean length as in the protobreccias and breccias (Fig. 5), but they have higher densities within individual fragments. There is no overall preferred orientation (Fig. 6).

Cataclasites from the Ord thrust plane

Approaching the Ord thrust plane from a distance of 25 m away, a similar sequence of microstructures can be observed from intact quartzite through protocataclasite to cataclasite and ultracataclasite on the thrust plane itself (Fig. 3f). This cataclasite sequence shows many of the same features as the breccia sequence: increasing microcrack density and progressive reduction of intact fragments to matrix. However, it is distinguished by a lack of overgrowths and iron oxide inclusions; there is also a weak foliation developed in the ultracataclasite, defined by fine grained white phyllosilicate minerals which are thought to represent new growths. Although Sibson (1977) defined cataclasites as non-foliated fault rocks, it has been acknowledged that cataclastic fault products often do possess a foliation; House & Gray (1982) found this to be the case with cataclasites along the Saltville thrust, and Chester *et al.* (1985) have also reported foliated cataclasites.

In an attempt to assess the possibility of intracrystalline plasticity contributing to the deformation, the range of extinction angle was measured for grains showing undulose extinction. One hundred grains were measured in samples of intact quartzite, protobreccia, breccia and ultrabreccia. Histograms of extinction angle ranges and means are shown in Fig. 9, indicating that no increase in undulose extinction occurs with progressively more intense deformation. The observed optical strain features are therefore probably inherited.

Table 1. Extension microcrack densities in Cambrian quartzites compared with some experimental data. Densities are calculated as the average of at least four randomly spaced traverses normal to the microcrack planes in thin sections. All experimental densities have been measured in a similar way

		Crack density (mm^{-1})	Conf. pressure (MPa)	Strain rate s^{-1}	Temperature (°C)	No. of measurements	Reference
Intact quartzite	32	6.82				500	This study
Protobreccia	11	5.72				500	
Protobreccia	10	14.5				500	
Protobreccia	8	17.3				500	
Breccia	6	36.0				500	
Oughtisbridge Ganister		2.61	200	10^{-5}	20	90	Hadizadeh (1980)
Westerly granite		4.91				182	Tapponier & Brace (1976)
		4.82				178	
		5.97				502	
		5.39				448	
		8.85				861	
		5.71				597	
		5.2	0	10^{-4}	24		Friedman & Logan (1970)
		5.5	100	10^{-2}	24		
		23.5	200	10^{-2}	24		
		13.5	300	10^{-2}	24		

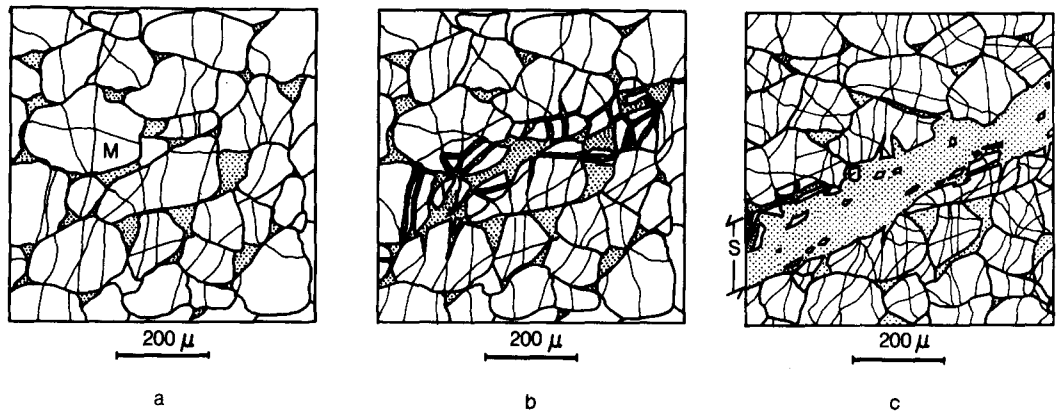

Fig. 8. The diagrammatic microstructural evolution of cataclasis in the Cambrian quartzites. (a) Development of intragranular extension microcracks (M) along σ_1–σ_2 planes by impingement. (b) Extension microcracks link and widen to form a small shear fault, shown in stipple. Microcrack density, but not length, increases. (c) The shear fault (S) widens and matrix is generated by reduction of grain fragments and cementation. The next stage (not illustrated) is localization of strain on much larger breccia zones.

THE DEFORMATION HISTORY OF THE QUARTZITE AND THE MOINE THRUST ZONE ON SKYE

Deformation mechanisms in the quartzite

It is proposed that the intact quartzite, protobreccia, breccia and ultrabreccia represent a sequence of progressive deformation which involves three processes that have some experimental analogues.

(1) *Development of extension microcracks.* The extension microcracks form in response to tensile stresses developed by impingement of grains at contact points in accordance with the principles of indentation fracture (Lawn & Wilshaw 1975). This is confirmed by the important demonstrations of Gallagher *et al.* (1974) and more recently McEwen (1981). In the former, photo-elastic studies of sand, glass, and resin models of aggregates of grains showed that extension microcracks followed faithfully the trajectories of maximum principal stress, producing similar geometries of cracks linking grain-to-grain contacts as noted in the Cambrian quartzites of the present study. McEwen's photoelastic experiments model the quartzites even more closely by allowing grain contacts along progressively more convexo-concave surfaces which arise from increasing amounts of pressure solution. The fact that mean crack lengths are always less than mean grain size (Fig. 5), and the good preferred orientation (Fig. 6) confirm that the extension microcracks formed in an identical way to those of the experiments, that is along principal stress surfaces from impingement points. Rotation of grains and microcracks clearly occurs in the subsequent stage of shear fault formation (see below).

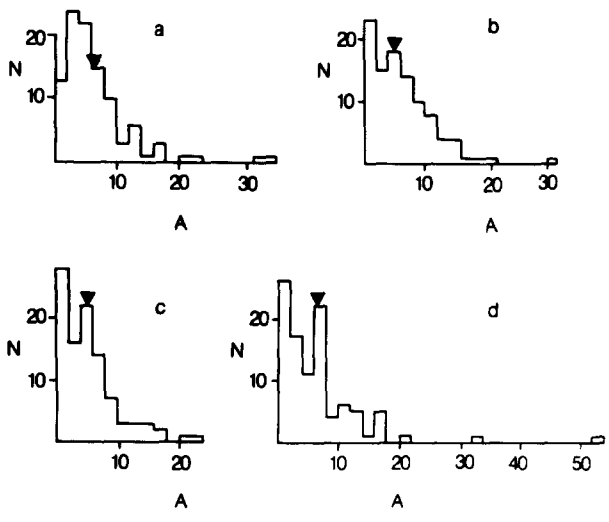

Fig. 9. Histograms of angle (A) between extinction positions. *N*, number of grains; triangle, mean value of A. 100 measurements for each sample. The mean value does not change significantly with deformation. (a) Intact quartzite (sample 32); (b) protobreccia (sample 11); (c) breccia (sample 6), and (d) ultrabreccia (sample 7). See Fig. 2 for sample locations.

Such extension microcracks have been recognized from the earliest experimental studies of cataclasis (e.g. Borg *et al.* 1960), where they are usually described as 'axial cracks'. They can begin to form in all experiments well before the peak stress, and are generally accepted as the dominant cause of: (a) prefailure dilatancy (Brace *et al.* 1966); (b) dilatancy hardening (Brace & Martin 1968); (c) the accumulation of brittle creep strains (Kranz 1979, Costin 1983) and (d) seismic velocity anisotropy (O'Connell & Budiansky 1974). Yet no previous reports of such high densities of naturally occurring *intragranular* extension microcracks are known, probably because they are so hard to identify without the use of CL.

Table 1 presents crack densities from the Cambrian quartzites compared to densities measured in a similar way in Oughtisbridge Ganister and Westerly granite, both deformed in the laboratory (Hadizadeh 1980, Tapponier & Brace 1976, Friedman & Logan 1970). The similarity in order of magnitude suggests that cataclastic failure may depend on a critical crack density as proposed, for example, by Kranz & Scholz (1977) and Costin (1983).

(2) *Development of shear faults.* Shear faults develop by linking of and shearing along extension microcracks, which isolate fragments of grains. These then continue to rotate and comminute to form part of the fine-grained matrix, as shown diagrammatically in Fig. 8. In addition to the comminuted debris of grains, the shear fault matrix consists of cement which itself often shows evidence of subsequent fracturing. It is therefore probable that cementation and cataclasis proceeded simultaneously. Polyepisodic movement on the shear faults can be demonstrated by the irregular distribution of iron oxides and the truncating relationships of one shear by another. Exactly such a cyclic deformation has been described in cataclasites by Stel (1981). Crack healing and cementation have been demonstrated experimentally to be relatively rapid (e.g. Smith & Evans 1984). Only a few days are required to fill cracks of the size observed and at the temperature inferred in this study following a dynamic faulting event. If crack growth was subcritical, cementation might reasonably be expected to match crack growth rates.

The formation of shear faults from the coalescence of microcracks is a well-known experimental feature. Peng & Johnson (1972) argued that for Chelmsford Granite, slivers bounded by axial cracks failed through buckling once a suitable aspect ratio was attained, thereby allowing a continuous planar fault zone to propagate in a series of steps throughout the specimen. Many subsequent experiments have confirmed that the final failure surface is formed by linking of early axial cracks (e.g. Hallbauer *et al.* 1973; Dunn *et al.* 1973).

The relative importance and timing of intra-, trans- and circum-granular microcracks in the formation of shear faults in rocks is probably strongly dependent on initial microstructure of the rocks (Hadizadeh 1980, Hadizadeh & Rutter 1982). Two extremes could be considered (Hadizadeh 1980). *Type 1.* Grains or crystals are not free to impinge on one another at contact points. This includes low porosity, well cemented and monomineralic crystalline rocks, in which the stress distribution is initially homogeneous throughout the rock. Because elastic modulus contrast effects between grains and indentation effects are lacking in such rocks, shear mode grain boundary cracking is favoured and axial cracking is suppressed until late in the loading history. A quartzite which was well cemented prior to loading would have this type of microstructure (e.g. Oughtisbridge Ganister, Hadizadeh & Rutter 1982). *Type 2.* Grains or crystals can impinge at contact points, due to lack of, or weak cement, or large elastic mismatches between constituents. This category includes rocks with high porosities, little or no cement, and large contrasts in elastic moduli between different grains (e.g. polyphase igneous rocks such as granite) or between grains and cement (for example where the cement is clay). The stress is markedly inhomogeneous, favouring intragranular axial cracks which may be cross-linked before or after formation by subordinate grain boundary cracks. The essential difference between the two microstructures is the initial distribution of stress on a grain scale. The abundant intragranular extension microcracks and a lack of evidence for circumgranular cracks or impingement cracks in the cement in the Cambrian quartzites suggests that at the time of deformation they were more similar to the Type 2 microstructure, that is the rock was a weakly cemented sandstone, and that the porosity was largely eliminated as a result of the cementation associated with and following the deformation events.

The shear faults of this study are closely comparable with the "braided shear fractures" of Engelder (1974), the "granulation seams" of Pittman (1981), the "microfaults" of Jamison & Stearns (1982), and the "deformation bands" of Aydin & Johnson (1983). All are zones of shear displacement less than 1 centimetre wide, with reduced porosity and fine grained matrix in otherwise porous sandstones (The Simpson Group, Wingate Sandstone, Navajo and Entrada Sandstones, respectively). These also presumably have a Type 2 microstructure.

(3) *Development of breccias and ultrabreccias.* The morphology of fragments within the breccias shows that the breccia zones evolved as large-scale analogues of the shear faults. Large fragments are initially isolated at the edges of breccia zones and progressively broken down to form matrix. At a smaller scale, the process is assisted by the continual development of intragranular extension microcracks, which have a weaker preferred orientation than in the protobreccias because of the larger rotations suffered by fragments in the breccia zone. The dilatancy concentrated fluid flow in the breccias to produce the overgrowths and iron oxides. The ultimate stage is the destruction of all fragments to form an ultrabreccia.

Breccia zone widths vary rapidly and non-systematically along strike, and displacement (d) and width (t) cannot be correlated. The large angle between oriented microcracks and the breccia zones suggests that only small resolved shear components acted along the breccia zones. Thus displacements might be expected to be small, as is in fact observed. Experiments by Engelder (1974) and Teufel (1981) suggested that gouge zone thickness increased with displacement, and Rutter (1979) showed that fault gouge thickness has a large effect on rheology of kaolinite fault gouges. Robertson (1983), on the basis of measurements along many normal, reverse and small thrust faults with comparable dimensions to the breccia zones of this study, inferred a linear d/t relationship. Robertson's data, however, cannot be taken to imply that an individual fault zone will develop a d/t relation similar to that displayed by the whole set, especially in view of the fact that no account was taken of variation in d/t relations along individual faults in compiling the data. Jamison & Stearns (1982) failed to find a d/t relationship for microfaults in the Wingate sandstone.

The sub-planar breccia zones cross-cut the fold structure (Fig. 2) and must therefore represent the last stage of deformation. This is also indicated by the lack of folding of the shear faults and breccia zones around the

fold axis (Fig. 7). The folding was mostly accommodated during the formation of the shear faults and the spread of the protobreccia texture throughout the quartzite. Following fold accommodation by processes 1 and 2, further strain became localized. The rock types and processes discussed above are summarized in Table 2.

Cataclasis in the evolution of the Moine thrust zone on Skye

Using Rf/ϕ techniques on the outcrop of pipes at the bedding surface of a fold in the Ord area, Potts (1982) showed that they recorded no bedding-parallel strain, and confirmed this result by palaeomagnetic strain determinations on the Torridonian Applecross formation in the Loch Eishort antiform. He concluded that flexural slip and rigid body rotation accommodated the folding in the limb, but raised the question of the apparent lack of deformation mechanisms in the fold hinge. The cataclastic deformation of the quartzite has been shown in this study to be a solution to this problem.

The Sgiath Bheinn Tokavaig fold is but one of a train of large folds which includes the Loch Eishort fold and the Loch Alsh synform, developed in association with overthrusting displacements onto the Caledonian foreland. Cataclasis accommodated both the recumbent folding and subsequent movement along the Ord thrust, and therefore probably took place both before and after the first movements on the Moine thrust.

DISCUSSION

The rock deformation perceived in this area involves cracking (brittle deformation) on a range of size scales. The folding is accommodated by distributed microcracking and small-scale shearing, which renders the rock macroscopically *ductile*, in the sense of the ability to accommodate large, non-localized strains (Stearns 1968). As defined by experimentalists (e.g. Paterson 1978, Rutter 1982), the concept of the brittle–ductile transition is from faulting to the same type of cataclastic flow as observed here. There is, however, a tendency amongst some geologists to restrict the concept of ductility to intracrystalline plastic deformation, so that the concept relates to a particular deformation mechanism, rather than being merely the capacity to accommodate a large non-localized strain, irrespective of mechanism. We suggest that the type of deformation observed here should be regarded as ductile, and that attempts to restrict the use of this term to a particular deformation mechanism will eventually lead to problems in the description and interpretation of the wide range of deformation features that rocks can display in nature, particularly under low-grade conditions.

It may be surmised that the hardening necessary to stabilize the deformation so that it spreads throughout the rock mass arises through the coeval cementation and healing of cracks. Localized, more intense cataclasis on a range of scales has also developed (small faults, breccia zones and the large thrusts). Such zones could develop at times when the rate of cementation failed to keep pace with the imposed deformation rates, or simply as a response to the material properties of the host rock mass having been changed through the initial microcracking–deformation history. Fluctuations in effective stress due to changes in pore water pressure would have the same effect. Our microstructural observations also support the view that in some instances recurrence times for present day seismic activity may reflect interrelationships between rate of application of tectonic stress and rate of hardening through cementation of fault rocks by circulating groundwater.

The effects of microstructural evolution on fault localization have been investigated, for example, by Rudnicki & Rice (1975) from a theoretical standpoint; and Aydin & Johnson (1983) have attempted to apply these ideas to the interpretation of the structural features of naturally deformed Entrada and Navajo sandstones. The conditions for localization are determined by the critical value of the strain hardening modulus, which in turn depends on the dilatancy, the elastic moduli and the coefficient of friction. These physical properties are clearly sensitive to the path of microstructural evolution during loading. The evidence of microcracking leading to shear faulting suggests that the dilatancy factor at the time of shear faulting was positive. For a positive dilatancy factor under a significant state of triaxial stress, Aydin & Johnson (1983) show that the Rudnicki & Rice model predicts that shear faults form while the rock is strain-softening well after peak stress, unlike the conditions inferred for the Entrada and Navajo sandstones.

Because of the geometrical similarity of natural *grain scale* microcracking observed in this study to microcracking observed in laboratory experiments on rocks with a 'Type 2' microstructure, we can roughly estimate the level of differential stress which may have been associated with the folding. The porosity of the Cambrian quartzites at the time of deformation is estimated as approximately 15%. Quartz sandstones of 10% porosity exhibit uniaxial strengths of 100 MPa, increasing to 200 MPa at 50 MPa and 350 MPa at 150 MPa effective confining pressure, respectively (Hoshino *et al.* 1972). Effective pressure must have been at least a few tens of MPa, because pervasive intragranular microcracking in sandstones is suppressed if pore pressure is increased to a level such that effective pressure approaches zero. Thus differential stress levels of the order of 150–250 MPa are indicated. Generally, cataclastic deformation is not markedly sensitive to either strain rate or temperature (Donath & Fruth 1971). This is reflected in (a) the strong sensitivity of subcritical crack growth rates to small changes in stress intensity factor and (b) low activation enthalpies for quartz crystals and quartz rocks (Atkinson 1982). The resistance to cataclastic flow of this rock is unlikely to be more than halved, even over a time scale of tens of millions of years at 200°C.

Table 2. A model for the cataclasis of Cambrian quartzites in the Sgiath Bheinn Tokavaig antiform

Rock type & sample	Proportion of matrix	Microstructures	Processes	Outcrop
Intact quartzite 32		Angular to subrounded grains, 0.2 mm diameter. Curved & interlocking grain boundaries. Some optical strain features and internal structures. A few extension microcracks.	A limited amount of pressure solution. Inherited strain and internal features. ?Some porosity reduction by pore collapse and grain boundary cracking/sliding.	Undeformed limb of Sgiath Bheinn Tokavaig antiform.
	0			
Protobreccia 8, 10, 11, 12		Extension microcracks in intact grains with densities 5–20 mm^{-1}.	Impingement and stress concentration of grain contacts. Microcracks form along σ_1–σ_2 planes.	Homogeneous distribution around hinge of fold.
		Shear faults 1–44 mm × 40–50 mm with displacements of tens of mm.		
		Fine grained non-luminescing matrix with grain fragments.	Linking and widening of microcracks to form plane of shear fault.	
			Comminution of grains and cementation. ?Syntectonic microcrack healing.	
	25%			
Breccia 6		Increased microcrack density (>20 mm^{-1}).	Further impingement microcracking.	Localized on discrete vertical planes 2–150 cm × 1–200 m, with displacement of m.
		Fragments of protobreccia in fine grained matrix.	Linking of shear belts to form breccia zones.	
		Increased proportion of iron oxides and cement.	Concentration of fluid flow in dilatant zones with deposition of oxides and cement.	
	75%			
Ultrabreccia 7		Smaller, more rounded fragments of protobreccia.	Almost complete destruction of fragments.	Locally along breccia zones.
		Further concentration of iron oxides.	Increased fluid flow.	

SUMMARY AND CONCLUSIONS

(1) An example of folding accommodated by pervasive cataclastic flow has been described. The cataclasis occurred by development of intragranular microcracks which linked to form a network of shear faults, and ultimately larger breccia zones.

(2) The local area studied displays examples of the cataclastic deformation mechanisms typically found at the southern end of the Moine thrust zone.

(3) Cathodoluminescence provides a powerful method of rendering visible cataclastic processes on a grain scale, which might otherwise be missed.

(4) Although two of the processes described have good experimental analogues, the natural cataclastic phenomena also occur at a much larger size scale than any experiments have been able to simulate. Caution is therefore required in extrapolating from experimental results to crustal scale deformation; this should only be done for scale-similar processes.

(5) The Rudnicki & Rice theory (1975), as applied to a natural situation by, for example, Aydin & Johnson (1983), offers a promising approach to understanding the parameters that have affected strain localization and history of the quartzites. Comparative investigations into the effect of initial microstructure and deformation on these parameters would be useful.

Acknowledgements—This study was carried out whilst the first author was the holder of a N.E.R.C. postgraduate studentship at Imperial College, University of London. We are indebted to Drs S. H. White and R. H. Sibson for their help and critical discussion, and to P. Grant and R. Giddens for SEM facilities. Assistance from college staff is gratefully acknowledged in the thin-section laboratory, sedimentology, X-ray and photography departments. Discussions with David Oliver, Dr R. G. Park and Dr N. J. Kuznir have contributed greatly, while Dr G. J. Potts made valuable observations on the field area. Finally, comments from two anonymous reviewers resulted in considerable improvements to the text.

REFERENCES

Atkinson, B. K. 1982. Subcritical crack propagation in rocks: theory, experimental results and applications. *J. Struct. Geol.* **4**, 41–56.

Aydin, A. & Johnson, A. M. 1983. Analysis of faulting in porous sandstones. *J. Struct. Geol.* **5**, 19–35.

Borg, I., Friedman, M., Handin, J. & Higgs, D. V. 1960. Experimental deformation of St. Peter Sand: a study of cataclastic flow. In: *Rock Deformation* (edited by Griggs, D. & Handin, J.). *Mem. geol. Soc. Am.* **79**, 133–192.

Brady, B. T. 1974. Theory of earthquakes—I. A scale of independent theory of rock failure. *Pure appl. Geophys.* **112**, 701–725.

Brace, W. F. & Martin, R. J. 1968. A test of the effective stress law for crystalline rocks of low porosity. *Int. J. Rock Mech. Min. Sci.* **5**, 415–426.

Brace, W. F., Paulding, D. W. Jr. & Scholz, C. H. 1966. Dilatancy in the fracture of crystalline rocks. *J. geophys. Res.* **71**, 3939–3953.

Brock, W. G. & Engelder, T. 1977. Deformation associated with the movement of the Muddy Mountain overthrust in the Buffington Window, southeastern Nevada. *Bull. geol. Soc. Am.* **88**, 1667–1677.

Butler, R. W. H. 1982. Hangingwall strain: a function of duplex shape and footwall topography. *Tectonophysics* **88**, 235–246.

Cheeney, R. F. & Matthews, D. W. 1965. The structural evolution of the Tarskavaig and Moine nappes in Skye. *Scott. J. Geol.* **1**, 256–281.
Chester, F. M., Friedman, M. & Logan, J. M. 1985. Foliated cataclasites. *Tectonophysics* **111**, 139–146.
Costin, L. S. 1983. A microcrack model for the deformation and failure of brittle rock. *J. geophys. Res.* **88**, 9485–9492.
Cruden, D. M. 1974. The static fatigue of brittle rock under uniaxial compression. *Int. J. Rock Mech. Min. Sci. & Geomech. Abstr.* **11**, 67–73.
Donath, F. A. & Fruth, L. S. 1971. Dependence of strain rate effects on deformation mechanism and rock type. *J. Geol.* **79**, 347–371.
Dunn, D. E., LaFountain, L. J. & Jackson, R. E. 1973. Porosity dependence and mechanism of brittle fracture in sandstones. *J. geophys. Res.* **78**, 2403–2417.
Engelder, J. T. 1974. Cataclasis and the generation of fault gouge. *Bull. geol. Soc. Am.* **85**, 1515–1522.
Friedman, M. & Logan, J. M. 1970. Microscopic feather fractures. *Bull. geol. Soc. Am.* **81**, 3417–3420.
Gallagher, J. J., Friedman, M., Handin, J. & Sowers, G. M. 1974. Experimental studies relating to microfractures in sandstone. *Tectonophysics* **21**, 203–247.
Hadizadeh, J. 1980. An experimental study of cataclastic deformation in a quartzite, Unpublished Ph.D. thesis, Imperial College, University of London.
Hadizadeh, J. & Rutter, E. H. 1982. Experimental study of cataclastic deformation of a quartzite. *Proc. 23rd. Symp. on Rock Mechanics*, University of California, Berkeley (edited by Goodman, R. E. & Heuze, F. E.) 372–379.
Hallbauer, D. K., Wagner, H. & Cook, N. G. W. 1973. Some observations concerning the microscopic and mechanical behaviour of quartzite specimens in stiff, triaxial compression tests. *Int. J. Rock Mech. Min. Sci.* **10**, 1853–1873.
Hoshino, K., Loide, H., Inami, K., Iwamura, S. & Mitsui, S. 1972. Mechanical properties of Japanese Tertiary sedimentary rocks under high confining pressure. *Report No.* 244, *Geol. Survey Japan*.
House, W. M. & Gray, D. R. 1982. Cataclasites along the Saltville thrust, U.S.A. and their implications for thrust sheet emplacement. *J. Struct. Geol.* **4**, 257–289.
Jamison, W. R. & Stearns, D. W. 1982. Tectonic deformation of Wingate Sandstone, Colorado National Monument. *Bull. Am. Ass. Petrol. Geol.* **66**, 2584–2608.
Kisch, H. J. 1983. Mineralogy and petrology of burial diagenesis (burial metamorphism) and incipient metamorphism in clastic rocks. In: *Diagenesis in Sediments and Sedimentary Rocks, 2.* (edited by Larsen, G. & Chilinger, G. V.) *Developments in Sedimentology, 25 B*, Elsevier, Amsterdam, 289–493.
Knipe, R. & White, S. H. 1979. Deformation in low grade shear zones. *J. Struct. Geol.* **1**, 283–297.
Kranz, R. L. 1979. Crack growth and development during creep of Barre granite. *Int. J. Rock Mech. Min. Sci.* **16**, 23–25.
Kranz, R. L. & Scholz, C. H. 1977. Critical dilatant volume of rocks at the onset of tertiary creep. *J. geophys. Res.* **82**, 4893–4897.
Lawn, B. & Wilshaw, R. 1975. Review of indentation fracture: principles and applications. *J. Mater. Sci.* **10**, 1049–1081.
Long, J. V. P. & Agrell, S. O. 1965. The cathodoluminescence of minerals in thin section. *Mineralog. Mag.* **34**, 318–326.
McClay, K. R. & Coward, M. P. 1981. The Moine Thrust Zone: an overview. In: *Thrust and Nappe Tectonics* (edited by McClay, K. & Price, N. J.). *Spec. Publs geol. Soc. Lond.* **9**, 241–260.
McEwen, T. J. 1981. Brittle deformation in pitted pebble conglomerates. *J. Struct. Geol.* **3**, 25–37.
Muir, M. D. & Holt, D. B. 1974. Analytical cathodoluminescence mode scanning electron microscopy. *Scanning Electron Microscopy*, 1974. Pt. 1 Proc. 7th Ann. S.E.M. Symp., Chicago, Illinois, I.I.T.R.I., 135–142.
O'Connell, R. J. & Budiansky, B. 1974. Seismic velocities in dry and saturated cracked solids. *J. geophys. Res.* **79**, 5412–5426.
Paterson, M. S. 1978. *Experimental Rock Deformation—The Brittle Field*. Springer, Berlin.
Pittman, E. D. 1981. Effect of fault-related granulation on porosity and permeability of quartz sandstones, Simpson Group, (Ordovician), Oklahoma. *Bull. Am. Ass. Petrol. Geol.* **65**, 2381–2387.
Peng, S. & Johnson, A. M. 1972. Crack growth and faulting in a cylindrical sample of Chelmsford Granite. *Int. J. Rock Mech. Min. Sci.* **9**, 37–86.
Potts, G. J. 1982. Finite strains within recumbent folds of the Kishorn Nappe, northwest Scotland. *Tectonophysics* **88**, 313–319.
Robertson, E. C. 1982. Continuous formation of gouge and breccia during fault displacement. *Proc. 23rd. Symp. on Rock Mechanics*. University of California, Berkeley. (edited by Goodman, R. E. & Heuze, F. E.) 397–404.
Robertson, E. C. 1983. Relationship of fault displacement to gouge and breccia thickness. *Min. Engng* **35**, 1426–1432.
Rudnicki, J. W. & Rice, J. R. 1975. Conditions for the localisation of deformation in pressure sensitive dilatant materials. *J. Mech. Phys. Solids* **53**, 371–394.
Rutter, E. H. 1979. The mechanical properties of kaolinite fault 'gouge' at moderate confining pressure, 20°C. *Int. J. Rock Mech. Min. Sci.* **16**, 407–410.
Sibson, R. H. 1977. Fault rocks and fault mechanisms. *J. geol. Soc. Lond.* **133**, 191–213.
Sibson, R. H. 1983. Continental fault structure and the shallow earthquake source. *J. geol. Soc. Lond.* **140**, 741–767.
Sipple, R. F. 1968. Sandstone petrology, evidence from luminescence petrography. *J. sedim. Petrol.* **38**, 530–554.
Smith, D. L. & Evans, B. 1984. Diffusional crack healing in quartz. *J. geophys. Res.* **89**, 4125–4135.
Smith, J. V. & Stenstrom, R. C. 1965. Electron-excited luminescence as a petrologic tool. *J. Geol.* **73**, 627–635.
Sommers, S. E. 1972. Cathodoluminescence of carbonates. *Chem. Geol.* **9**, 257–284.
Sprunt, E. S., Dengler, L. A. & Sloan, D. 1978. Effects of metamorphism on quartz cathodoluminescence. *Geology* **6**, 305–308.
Sprunt, E. S. & Nur, A. 1979. Microcracking and healing in granites: new evidence from cathodoluminescence. *Science, Wash.* **205**, 495–497.
Stearns, D. W. 1968. Fracture as a mechanism of flow in naturally deformed layered rocks. *Geol. Surv. Pap. Can.* **68–52**, 68–80.
Stel, M. 1981. Crystal growth in cataclasites: diagnostic structure and implications. *Tectonophysics* **78**, 585–600.
Tapponier, P. & Brace, W. F. 1976. Development of stress induced microcracks in Westerly granite. *Int. J. Rock Mech. Min. Sci.* **13**, 103–112.
Teufel, L. W. 1981. Pore volume changes during frictional sliding of simulated faults. In: *Mechanical Behavior of Crustal Rocks*. (edited by Carter, N. L., Friedman, M., Logan, J. M. & Stearns, D. W.), *Am. Geophys. Un. Monogr.* **24**, 135–145.
White, S. H. 1976. The effects of strain on the microstructures, fabrics, and deformation mechanisms in quartzites. *Phil. Trans. R. Soc.* **A283**, 69–86.
Wilkins, B. J. S. 1980. Slow crack growth and delayed failure of granite. *Int. J. Rock. Mech. Min. Sci. Geomech. Abstr.* **17**, 365–369.
Wise, D. U., Dunn, D. E., Engelder, J. T., Geiser, P. A., Hatcher, R. D., Kish, S. A., Odom, A. L. & Schamel, S, 1984. Fault-related rocks: some suggestions for terminology. *Geology* **12**, 391–394.
Zinkernagel, V. 1978. Cathodoluminescence of quartz and its application to sandstone petrology. *Contr. Sediment.* **8**, 1–6.